International Journal of Industrial Engineering Computations 10 (2019) 535–556

Contents lists available at GrowingScience

International Journal of Industrial Engineering Computations

homepage: www.GrowingScience.com/ijiec

Optimal placement of freight electric vehicles charging stations and their impact on the power distribution network

Andrés Arias Londoño[a] and Mauricio Granada-Echeverri[a*]

[a]*Universidad Tecnológica de Pereira, Colombia*

C H R O N I C L E

Article history:
Received August 28 2018
Received in Revised Format February 7 2019
Accepted March 15 2019
Available online March 15 2019

Keywords:
Electric vehicle
Capacitated vehicle routing problem
Shortest path problem
Transportation network
Power distribution system
Electric vehicle charging station

A B S T R A C T

In this paper, an optimization model for the Charging Station Location Problem of Electric Vehicles for Freight Transportation CSLP-EVFT is presented. This model aims to determine an optimal location strategy of Electric Vehicle Charging Stations EVCSs and the routing plan of a fleet of electric vehicles under battery driving range limitation, in conjunction with the impact on the power distribution system. Freight transportation is modeled under the mobility patterns followed by the Capacitated Vehicle Routing Problem CVRP for contracted fleet, and Shortest Path SP problem for subcontracted fleet. A linear formulation of the power flow is used in order to consider the impact on the electric grid. Several costs are examined, i.e., EVs routing, installation and energy consumption of EVCSs, and energy losses. Although uncertainties related to temporal variation of some aspects (number of customers and their demands, fleet size, power network nodes and routes) are not addressed, the proposed model represents a useful approach to evaluate multiple scenarios or to be introduced within stochastic optimization. Instead, the mathematical model is studied under the variation of EVs travel range that accounts for the advance of battery technology and sensitivity analysis. Additionally, the problem is reduced to a mixed integer non-linear mathematical model, which is linearized by using multivariable Taylor's series.

Nomenclature

Sets:

N	Set of customers on the transportation network
K	Set of vehicles in the CVRP formulation
E	Set of vehicles in the SP formulation
C	Set of candidate points to install EVCS

Parameters

$\|K\|$	Number of vehicles for CVRP

* Corresponding author
E-mail: magra@utp.edu.co (M. Granada-Echeverri)

2019 Growing Science Ltd.
doi: 10.5267/j.ijiec.2019.3.002

D_c	Demand of merchandise at customer c
Cap	Vehicle cargo capacity
S_e	Start nodes for routes traveled by vehicles in SP problem
E_e	End nodes for routes traveled by vehicles in SP problem
$d_{c,o}$	Distance from node c to node o [km]
$d_{d,p}$	Distance from node d to node p [km]
V^{nom}	Nominal voltage of the distribution system [V]
$S^{p}_{n_{a,b,c}}$	Constant power load at electrical node n [W]
$S^{i}_{n_{a,b,c}}$	Constant current load at electrical node n [W]
$S^{z}_{n_{a,b,c}}$	Constant impedance load at electrical node n [W]
$T_{a,b,c}$	Three-phase unit vector
C^{travel}	Cost per kilometer traveled [USD/km]
C^{main}	Maintenance cost in terms of kilometers traveled [USD/km]
FA	Factor of annualization
nt	Number of years in which the operation is considered (routing and energy consumption)
CPI	Consumer Price Index
C^{const}	Construction cost of EVCS [USD]
P^{bat}	Nominal power of EVCS [W]
Q^{cvrp}	Battery autonomy of the vehicles in CVRP [km]
Q^{sp}	Battery autonomy of the vehicles in SP problem [km]
CE	Cost of energy [USD/kWh]
$\overline{Loss}$	Power losses in the distribution system without electric vehicles (Benchmark case) [W]
$V^{s}_{a,b,c}$	Three-phase voltage at slack node [V]

Variables

$Y^{visit}_{c,k}$	Binary decision variable for CVRP with value of *1* if vehicle k visits the customer at transportation node c, and *0* otherwise
$x_{c,o,k}$	Binary decision variable for CVRP, with value of *1* if vehicle k goes from node c to node o of the transportation network and *0* otherwise
$t_{c,o}$	Remaining merchandise to be delivered at arc c,o
$y_{d,p,e}$	Binary decision variable in SP problem, taking the value of *1* if vehicle e goes from node d to node p and *0* otherwise
$d^{cvrp}_{c,k}$	Distance traveled at node c by vehicle k in CVRP [km]
$d^{\overline{cvrp}}_{o,k}$	Auxiliar variable for distance traveled at node o by vehicle k in CVRP [km]
Y^{cvrp}_{o}	Binary decision variable in CVRP, taking the value of *1* if an EVCS is installed at node o, and *0* otherwise
$d^{sp}_{d,e}$	Distance traveled at node d by vehicle e in SP problem [km]
$Y^{sp}_{p,e}$	Binary decision variable in SP problem, taking the value of *1* if an EVCS is installed at node p for EV e, and *0* otherwise

$d_{o,e}^{\overline{sp}}$	Auxiliar variable for distance traveled at node o by vehicle e in SP problem [km]
U_v	Unification variable for Y_o^{cvrp} and $Y_{p,e}^{sp}$
$I_{a,b,c}^{s}$	Three-phase current at slack node [A]
$I_{a,b,c}^{n}$	Three-phase current at electrical node n other than the slack node [A]
$V_{a,b,c}^{n}$	Three-phase voltage at electrical node n other than the slack node [V]
$Loss$	Power losses in the distribution system [W]

1. Introduction

One of the greatest obstacles for the massive adoption of Electric Vehicles (EVs) is their limited autonomy compared with the internal combustion engines. The majority of the vehicles in 2017 had autonomies (considering fully charged batteries) ranging from 100 km to 400 km (Schmidt, 2017), subject to weather conditions, traffic congestion and road topology. This range is not sufficient for all-electric vehicles to be considered as a primary mode of transportation and creates in drivers a feeling known as "range anxiety", which addresses the concern of EV's driver to reach a critical level on the battery before arriving to a charging station (Sarrafan et al., 2016).

On the other hand, the increasing introduction of EVs could have a large impact on the power distribution system, e.g., non-desired demand peaks and violations in the allowable voltage limits as a consequence of the simultaneous charging of batteries. Likewise, the power quality could be reduced by the introduction of harmonics on voltages and currents, due to the power-electronics-based charging infrastructure (Carradore & Turri, 2011). Other effects generated by the introduction of EVs in the power network are the congestion on feeders and transformers, overloading, and increment of power losses during charging of batteries. From the power system operator stand point, economic aspects, power quality, reliability, and power losses must be considered (Clement-Nyns et al., 2010).

Research on Electric Vehicle Charging Stations EVCSs has increased considerably in recent years. This is due to the intrinsic characteristics of the model which encourages academic research, but also due to practical reasons, since inadequate planning transportation networks and power distribution systems result in inefficient use of the infrastructure and high cost in charging stations (Zhang et al., 2017).

In this paper, the Charging Station Location Problem of Electric Vehicles for Freight Transportation CSLP-EVFT is presented, under the mobility patterns of freight EVs along the transportation network. This model is different from previous research in two main aspects: First, the optimal location of EVCSs is performed, considering the impact on the power distribution system PDS. Second, travel patterns are focused on the mobility behavior of contracted and subcontracted fleet, which are framed respectively into the Capacitated Vehicle Routing Problem CVRP and the Shortest Path SP problem. A mixed integer linear mathematical model is proposed to portray the freight EVs travel patterns and the operation of the distribution system; the latter is achieved by using a novel power flow formulation presented in (Garces, 2016) which allows to include the effect of the grid by an affine constraint. This study is motivated by the low capacity that may be presented on the EVs' battery to provide enough autonomy to complete routes successfully, since the freight EVs are required to travel very long distances too often. EVCSs provide a virtual increase on EV´s autonomy in case this latter is close to be depleted, warranting the deliveries to all the customers. On the other hand, the proper location of the EVCSs, represents a critical aspect when the energy losses of the PDS are addressed since these loads draw large quantities of energy during EV charging.

The remainder of this paper is organized as follows. In Section 2, the literature review around EVCSs planning is performed. Section 3 presents the mathematical model of the CSLP-EVFT problem, involving the freight EVs mobility patterns and the power network. The test systems, product of the combination of CVRP instances and IEEE distribution test feeders are shown in Section 4. The assessment results of CSLP-EVFT are presented in Section 5. Finally, conclusions are discussed in Section 6.

2. Literature review

In the specialized literature, many papers address the EVCSs planning along the power distribution system but few works include the transportation network. To the best of the authors knowledge, this subject started to be studied in 2010, where a two steps model was presented (Ip, Fong, (IMS), 6th, & 2010, n.d.). This model identified clusters of data points that represent the traffic concentrations on urbanized areas, and then applied optimization techniques over the clusters for meeting the supplies and demands. Subsequently, in (Luo et al., 2011) the Grey prediction model to forecast the electric vehicles ownership and the total count of the charging infrastructure was presented, considering the service radius and planning area. Similar to (Luo et al., 2011), in (Xie et al., 2011) a daily load forecasting model for EV charging station load was introduced, using Back-propagation and Radial Basis Function neural network and Grey prediction model. Taking into account the charging and trip characteristics of the EVs, in (Cui et al., 2014) a model of charging station planning for EVs was proposed along with the power distribution system, combining particle swarm optimization and weighted Voronoi diagram to find a solution. A more structured model was presented in (Hu & Song, 2012), which relates the distribution expansion planning with the siting and sizing of EVs charging stations, meeting charging demands with the lowest investment costs and best user's convenience. Similarly, in (Moradijoz & Moghaddam, 2012) the optimal allocation of parking lots providing Vehicle to Grid (V2G) power for loss reduction was studied, and (Feng et al., 2012a,b) presented a method for charging station location based on sensitivity analysis.

The integrated cost of investment and operation of the EV charging stations are key components involved in objective functions of mathematical models shown in (Jia et al. 2012) and (Liu et al., 2012). These studies are in compliance with the following principles: Charging station distribution is in keeping with charging demand distribution and traffic flow as far as possible; and the planning of the charging station should satisfy city's overall planning and road network planning requirements, as well as take the future development trend of EV in consideration. Other approaches include queuing theory to minimize the sum of customers waiting fees and charging stations' service cost (Feng et al., 2012b). From the point of view of transportation models, the work depicted in (Worley, 2012) and published in 2012, is one of the first papers that formulated the problem of charging stations location and designing EV routes, based on the classic CVRP. However, during 2013 and part of 2014, the studies continued to be driven in most of the cases considering the power distribution network rather than the transportation models, e.g., CVRP. That is the case of (Su et al., 2013) where the charging stations placement optimization is developed under the behavior of daily time varying loads together with EVs charging patterns, i.e., starting time, duration and power of charging. The system losses are minimized subject to system operation constraints. Another case is the work published in (Liu et al., 2013), which implements a two-step method consisting on: identify the candidate sites for charging stations, considering the environmental factors and service radius, and, solve a mathematical model using modified primal-dual interior point algorithm. This mathematical approach encompasses the total cost associated with EV charging stations to be planned, investment, operation and maintenance costs, as well as network loss in the planning period. Related works are found in (Neyestani et al., 2015) and (Aghaebrahimi et al., 2014), tackling allocation of EVs parking lots PL from the deterministic and probabilistic approach, taking into account the network reliability and voltage deviation, and the market interactions to provide profit to the PL owner. By the other side, in (Zheng et al., 2014) the appropriate placement of charging/swap stations is performed together with the reinforcement of distribution network by using differential evolution algorithm.

After the publication of (Worley et al., 2012), the transportation network was not considered until 2014 with the study performed by the authors of (Pourazarm et al., 2014), in which the optimal routing of electric vehicles in networks with charging nodes is addressed with dynamic programming. The vehicle total traveling time minimization problem in a transportation network containing inhomogeneous charging nodes is studied.

The deployment of different distributed generations DG, based on renewable and non-renewable resources, is not an alien subject to EVs charging stations planning on power distribution systems. These interactions (DG and charging stations planning) are considered in (Neyestani et al., 2014) and (Pazouki, Mohsenzadeh, Ardalan, & Haghifam, 2015) (the latter published in 2015), under the context of financial (investment costs), technical (system reliability, power loss and voltage profile) and environmental (CO_2 emissions) issues. As in (Pazouki et al., 2015), the study presents optimal planning of charging stations in distribution systems in presence of capacitors. Moreover, a better-structured formulation is proposed in (Abapour et al., 2015), maximizing the distribution system manager DSM benefit. According to this benefit and technical indices for the optimally located and sized charging stations, data envelopment analysis DEA is implemented to rank the stations found. The final charging stations are installed with the best rank for efficient planning.

In 2016, the transportation network is newly included with CVRP formulation for EVs (Yang et al., 2017). Although this study is not specifically involved with EV charging stations allocation planning, its relevance is framed on the operational planning approach with intelligent charging/discharging strategies in microgrids. In this manner, coordinated dispatch schemes of EVs are used to smooth renewable energy and load fluctuations while ensuring the quality of logistics services. Furthermore, over the course of that period (2016), other outstanding works were published, with greater emphasis of the EVs charging stations planning along the power distribution system and road network, thought without using CVRP formulation. For example, the study presented in (Wang et al., 2017) uses a multi-objective evolutionary algorithm to find the non-dominated solutions of a proposed collaborative planning model, which aims to minimize the investment and operation costs of the distribution system while maximize the annually captured traffic flow.

Without considering power grid, important contributions are shown by (del Razo & Jacobsen, 2016), where a smart scheduling approach for EVs to plan charging stops on a highway with limited charging infrastructure is proposed, in order to reduce the total travel times. In addition to this study, in (Zhang, Hu, Xu, & Song, 2016) different types of charging facilities are planned along roadside and public areas. Then, the forecasting of the spatial and temporal distribution of EVs charging load is developed, using EVs driving parking behaviors (from real-travel survey data), charging type, arrival time and parking duration. In the next year (2017), similar to Zhang et al. (2016), in Arias et al. (2017) the variation of energy price and probabilistic behavior of charging and driving patterns are considered, under the concept of priority periods. Other works are within the framework of freight transportation with EVs, such as Arias et al. (2017) and Toro et al. (2017).

According to the works mentioned above, the EVCSs planning in transportation networks and power distribution systems has been little investigated simultaneously, resulting in a real problem for the logistics firm and network operators. This work assumes that the transportation company and the distribution system belong to the same owner, as objective functions and constraints of both networks are in the same mathematical model. Otherwise, the problem should be handled considering a bi-level approach, being the routing solution and EVCSs location, the input to find the energy consumption and energy losses with the power flow formulation.

Contributions of this paper are summarized as follows: first, a new problem called CSLP-EVFT is proposed for optimal locating of EVCSs along the power distribution system and transportation network, finding optimal routes for contracted and subcontracted fleet conformed by EVs for freight transportation. Second, besides the Capacitated Vehicle Routing Problem CVRP, the Shortest Path SP problem is introduced, to model EVs path that follows the route from a start point towards an end point throughout the transportation network. Third, the operation with minimum power losses is evaluated by using a linear approach for the power flow on the distribution system. And finally, consistent test systems are proposed, which combine the CVRP instances and power distribution test feeders from the specialized literature.

3. CSLP-EVFT mathematical formulation

The CSLP-EVFT problem is divided into three subproblems: the CVRP and SP models for the mobility patterns in the merchandise transportation, the strategy for optimal location of EVCSs, and the linear formulation of power flow equations in the distribution system. All of them are combined in a mathematical model, which is explained in the following subsections.

3.1. Capacitated Vehicle Routing Problem (CVRP)

Vehicles utilized in merchandise transportation, are in accordance with the mobility patterns assigned by the CVRP. This implies that a fleet of vehicles with limited cargo capacity leaves from a unique depot, deliver merchandise to several customers and come back to depot, following the behavior of a contracted fleet (belonging to the depot owner). The vehicles have to fully meet the merchandise demands, seeking a travelling minimal cost (Toth et al., n.d.). Equations (1) to (10) represent the CVRP formulation, taking into consideration a fixed number of EVs in the problem.

$$\sum_{k\in K} Y_{c,k}^{visit} = 1 \qquad \forall c \in N \setminus \{Dep\} \tag{1}$$

$$\sum_{c\in N}\sum_{k\in K} x_{c,o,k} = 1 \qquad \forall o \in N \setminus \{Dep\} \tag{2}$$

$$\sum_{c\in N}\sum_{k\in K} x_{o,c,k} = 1 \qquad \forall o \in N \setminus \{Dep\} \tag{3}$$

$$\sum_{k\in K}\sum_{o\in N} x_{Dep,o,k} = |K| \tag{4}$$

$$\sum_{k\in K}\sum_{o\in N} x_{o,Dep,k} = |K| \tag{5}$$

$$\sum_{o\in N} x_{o,c,k} = Y_{c,k}^{visit} \qquad \forall c \in N \;\; \forall k \in K \tag{6}$$

$$\sum_{\substack{q\in N\\ c\neq q}} t_{q,c} = \sum_{\substack{o\in N\\ c\neq o}} t_{c,o} + D_c \qquad \forall c \in N \setminus \{Dep\} \tag{7}$$

$$\sum_{\substack{c\in N\\ c\neq Dep}} t_{Dep,c} = \sum_{\substack{c\in N\\ c\neq Dep}} D_c \tag{8}$$

$$t_{c,o} \le \sum_{k\in K} Cap \cdot x_{c,o,k} \qquad \forall c \in N,\;\; \forall o \in N \tag{9}$$

$$t_{c,Dep} = 0 \qquad \forall c \in N \setminus \{Dep\} \tag{10}$$

Eq. (1) imposes that one vehicle is assigned to one customer. Eqs. (2-3) are indegree and outdegree constraints, which impose that exactly one arc enters and leaves each vertex associated with each customer, respectively. Similarly, Eq. (4) and Eq. (5) show the degree requirements for the depot vertex (*Dep*), e.g., the number of vehicles leaving the depot has to be the same as the number of vehicles entering the depot. Eq. (6) avoids the visit to a customer by several vehicles. The flow of merchandise through each arc is tracked by Eq. (7). In Eq. (8) the summation of the flows of merchandise leaving the depot should be equal to the total customers demand to be delivered. Eq. (9) denotes that the remaining merchandise flowing through each arc is less than the cargo capacity of the vehicle. In Eq. (10), the remaining merchandise to be delivered is null just before completing the route.

3.2. Shortest Path (SP) problem

Other modes of freight transportation are developed in accordance with the SP problem, in which the vehicles have to travel from a start point to an end point, minimizing the travel distance (Pallottino & Scutellà, 1998). This mode of transportation is in accordance with the subcontracted fleet, as the transportation company is only pending that merchandise is delivered at the destination point, no matters how or which route the vehicle (belonging to the subcontracted fleet) takes to come back to the start point. Eq. (11) to Eq. (13) depict the SP formulation, considering a fixed number of vehicles.

$$\sum_{p\in N} y_{d,p,e} - \sum_{p\in N} y_{p,d,e} = 1 \qquad \forall d\in N,\ \forall e\in E,\ d=S_e \tag{11}$$

$$\sum_{p\in N} y_{d,p,e} - \sum_{p\in N} y_{p,d,e} = 0 \qquad \forall d\in N,\ \forall e\in E,\ d\neq S_e,\ d\neq E_e \tag{12}$$

$$\sum_{p\in N} y_{d,p,e} - \sum_{p\in N} y_{p,d,e} = -1 \qquad \forall d\in N,\ \forall e\in E,\ d=E_e \tag{13}$$

Eq. (11) imposes that only one arc leaves from the start point of the route. In Eq. (12) the number of arcs leaving from an intermediate node has to be the same as the number of arcs entering the node. Eq. (13) details that only one arc enters the end point of the route.

3.3. EVCSs location for CVRP problem

The EVCSs planning is related with the optimal location of these infrastructures along the transportation network. A key element on the EVCSs location is the battery autonomy consumption which is in terms of the distance being traveled on the route. Eq. (14) describes the distance traveled at any node other than the depot and the candidate nodes to charging stations.

$$x_{Dep,o,k}\cdot d_{Dep,o} + \sum_{\substack{c\in N\\ c\neq Dep\\ c\neq o}} x_{c,o,k}\cdot\left(d_{c,o} + d^{cvrp}_{c,k}\right) = d^{cvrp}_{o,k} \qquad \forall o\in N,\ \forall k\in K,\ o\neq Dep,\ o\notin C \tag{14}$$

Notice that one of the expressions involved in Eq. (14) is a non-linear term, i.e., the product between a binary variable and continuous variable, $x_{c,o,k}\cdot d^{cvrp}_{c,k}$. This latter is linearized according to the mathematical approach depicted in (15), replacing the product $x_{c,o,k}\cdot d^{cvrp}_{c,k}$ by $gl^{cvrp}_{c,o,k}$. In Eq. (16), the distance accumulated at node *c* is assigned to vehicle *k* for the arc *(c,o)*.

$$\left|gl_{c,o,k} - d^{cvrp}_{c,k}\right| \le Q^{cvrp}\cdot\left(1-x_{c,o,k}\right) \qquad \forall c\in N,\ \forall o\in N,\ \forall k\in K,\ c\neq Dep \tag{15}$$

$$gl^{cvrp}_{c,o,k} \le Q^{cvrp}\cdot x_{c,o,k} \qquad \forall c\in N,\ \forall o\in N,\ \forall k\in K,\ c\neq Dep \tag{16}$$

Eq. (15) is equivalent to the expression in Eq. (17), considering the absolute value definition.

$$-Q^{cvrp}\cdot\left(1-x_{c,o,k}\right)\le gl_{c,o,k}^{cvrp}-d_{c,k}^{cvrp}\le Q^{cvrp}\cdot\left(1-x_{c,o,k}\right) \qquad \forall c\in N,\ \forall o\in N,\ \forall k\in K,\ c\neq Dep \qquad (17)$$

In this sense, Eq. (14) is written in a linear form as shown in Eq. (18).

$$x_{Dep,o,k}\cdot d_{Dep,o}+\sum_{\substack{c\in N\\ c\neq Dep\\ c\neq o}} x_{c,o,k}\cdot d_{c,o}+gl_{c,o,k}^{cvrp}=d_{o,k}^{cvrp} \qquad \forall o\in N,\ \forall k\in K,\ o\neq Dep,\ o\notin C \qquad (18)$$

The distance traveled at the depot once the route is completed, is given by Eq. (19).

$$\sum_{\substack{c\in N\\ c\neq Dep}} x_{c,Dep,k}\cdot d_{c,Dep}+gl_{c,Dep,k}^{cvrp}=d_{Dep,k}^{cvrp} \qquad \forall k\in K \qquad (19)$$

The installation of an EVCS at the transportation node, involves the resetting of distance traveled so far, which is reflected in making zero the value of $d_{o,k}^{cvrp}$. Note in Eq. (20) that when an ECVS is installed ($Y_o^{cvrp}=1$), the variable $d_{o,k}^{cvrp}$ is reset. If $Y_o^{cvrp}=0$, then the Eq. (20) keeps valid.

$$d_{o,k}^{cvrp}\le\left(1-Y_o^{cvrp}\right)\cdot Q^{cvrp} \qquad \forall o\in C,\ \forall k\in K,\ o\neq Dep \qquad (20)$$

An auxiliary variable $\overline{d_{o,k}^{cvrp}}$ for the distance traveled $d_{o,k}^{cvrp}$ is required to avoid a conflict when the EVCS is installed and $d_{o,k}^{cvrp}$ becomes null. Eq. (21) shows $\overline{d_{o,k}^{cvrp}}$, which is calculated for all the nodes of the transportation network.

$$x_{Dep,o,k}\cdot d_{Dep,o}+\sum_{\substack{c\in N\\ c\neq Dep\\ c\neq o}} x_{c,o,k}\cdot d_{c,o}+gl_{c,o,k}^{cvrp}=\overline{d_{o,k}^{cvrp}} \qquad \forall o\in N,\ \forall k\in K \qquad (21)$$

Eq. (22) synchronizes the connection between $d_{o,k}^{cvrp}$ and $\overline{d_{o,k}^{cvrp}}$. If, $Y_o^{cvrp}=0$ (non-installation of an EVCS), the variables $d_{o,k}^{cvrp}$ and $\overline{d_{o,k}^{cvrp}}$ are equal, otherwise, the equation keeps valid.

$$\left|\overline{d_{o,k}^{cvrp}}-d_{o,k}^{cvrp}\right|\le Q^{cvrp}\cdot Y_o^{cvrp} \qquad \forall o\in C,\ \forall k\in K,\ o\neq Dep \qquad (22)$$

Eq. (22) is equivalent to Eq. (23), in accordance with absolute value definition.

$$-Q^{cvrp}\cdot Y_o^{cvrp}\le\overline{d_{o,k}^{cvrp}}-d_{o,k}^{cvrp}\le Q^{cvrp}\cdot Y_o^{cvrp} \qquad \forall o\in C,\ \forall k\in K,\ o\neq Dep \qquad (23)$$

In Eq. (24) and Eq. (25) the values for both $d_{c,k}^{cvrp}$ and $\overline{d_{c,k}^{cvrp}}$ should not be greater than the battery autonomy Q^{cvrp}. Equation (26) specifies the non-negativity of the EVCSs to be installed.

$$d_{c,k}^{cvrp}\le Q^{cvrp}\cdot Y_{c,k}^{visit} \qquad \forall c\in N,\ \forall k\in K,\ c\neq Dep \qquad (24)$$

$$\overline{d_{c,k}^{cvrp}}\le Q^{cvrp}\cdot Y_{c,k}^{visit} \qquad \forall c\in C,\ \forall k\in K,\ c\neq Dep \qquad (25)$$

$$\sum_{c\in C} Y_c^{cvrp}\ge 0 \qquad (26)$$

3.4. EVCSs location for SP problem

For the EVs that follow the SP problem, the EVCSs location is quite similar to the strategy treated for CVRP, except that in this case there is no depot due to the nature of SP problem, instead, the start point for the EV's route is considered.

The distance traveled at any node is depicted in Eq. (27), since the node is not a candidate for charging station. However, the presence of the non-linearity $y_{d,p,e} \cdot d^{sp}_{d,e}$ leads to the linearization in Eq. (28), being $gl^{sp}_{d,p,e}$ the variable that replaces this product. Eq. (28) is equivalent to Eq. (29) due to the absolute value concept. In (30), the distance accumulated at node *d* is assigned to the vehicle *e* for the arc *d,p*.

$$\sum_{\substack{d\in N\\ d=S_e}} y_{d,p,e} \cdot d_{d,p} + \sum_{\substack{d\in N\\ d\neq S_e}} y_{d,p,e} \cdot \left(d_{d,p} + d^{sp}_{d,e}\right) = d^{sp}_{p,e} \qquad \forall p\in N,\ \forall e\in E,\ p\notin C \qquad (27)$$

$$\left|gl^{sp}_{d,p,e} - d^{sp}_{d,e}\right| \le Q^{sp} \cdot \left(1 - y_{d,p,e}\right) \qquad \forall d\in N,\ \forall p\in N,\ \forall e\in E,\ d\neq S_e \qquad (28)$$

$$-Q^{sp} \cdot \left(1 - y_{d,p,e}\right) \le gl^{sp}_{d,p,e} - d^{sp}_{d,e} \le Q^{sp} \cdot \left(1 - y_{d,p,e}\right) \qquad \forall d\in N,\ \forall p\in N,\ \forall e\in E,\ d\neq S_e \qquad (29)$$

$$gl^{sp}_{d,p,e} \le Q^{sp} \cdot y_{d,p,e} \qquad \forall d\in N,\ \forall p\in N,\ \forall e\in E,\ d\neq S_e \qquad (30)$$

In this sense, Eq. (27) is replaced by Eq. (31).

$$\sum_{\substack{d\in N\\ d=S_e}} y_{d,p,e} \cdot d_{d,p} + \sum_{\substack{d\in N\\ d\neq S_e}} y_{d,p,e} \cdot d_{d,p} + gl^{sp}_{d,p,e} = d^{sp}_{p,e} \qquad \forall p\in N,\ \forall e\in E,\ p\notin C \qquad (31)$$

Eq. (32) performs the resetting of $d^{sp}_{p,e}$ when the EVCS is installed.

$$d^{sp}_{p,e} \le \left(1 - Y^{sp}_{p,e}\right) \cdot Q^{sp} \qquad \forall p\in C,\ \forall e\in E \qquad (32)$$

For the distance traveled $d^{sp}_{p,e}$, an auxiliary variable $d^{\overline{sp}}_{p,e}$, computed in Eq. (33), is also necessary to avoid a mathematical conflict when the EVCS is installed and $d^{sp}_{p,e}$ becomes null. See in Eq. (34) the non-negativity of the number of EVCSs installed for the EVs that follow the SP mobility patterns.

$$\sum_{\substack{d\in N\\ d=S_e}} y_{d,p,e} \cdot d_{d,p} + \sum_{\substack{d\in N\\ d\neq S_e}} y_{d,p,e} \cdot d_{d,p} + gl^{sp}_{d,p,e} = d^{\overline{sp}}_{p,e} \qquad \forall p\in N,\ \forall e\in E \qquad (33)$$

$$\sum_{d\in C} \sum_{e\in E} Y^{sp}_{d,e} \ge 0 \qquad (34)$$

3.5. Unifying variables of EVCSs installation

As noticed before, the installation of EVCSs is treated separately for CVRP and SP problems, due to the difference in EVs travel behaviors for each approach. With this in mind, both, Y^{cvrp}_{c} and $Y^{sp}_{d,e}$ are merged into U_v in order to represent the installation of charging stations of EVs that follow either the CVRP or the SP focuses. This unification is carried out in Eqs. (35-37).

$$\sum_{\substack{p\in N\\ p=v}} Y^{sp}_{p,e} - 1 \le U_v - 1 \le -\sum_{\substack{p\in N\\ p=v}} Y^{sp}_{p,e} + 1 \qquad \forall v\in N,\ \forall e\in E \qquad (35)$$

$$\sum_{\substack{c\in N\\ c=v}} Y^{cvrp}_{c} - 1 \le U_v - 1 \le -\sum_{\substack{c\in N\\ c=v}} Y^{cvrp}_{c} + 1 \qquad \forall v\in N \qquad (36)$$

$$-\sum_{\substack{c\in N\\ c=v}} Y^{cvrp}_{c} - \sum_{\substack{p\in N\\ p=v}} \sum_{e\in E} Y^{sp}_{p,e} \le U_v \le \sum_{\substack{c\in N\\ c=v}} Y^{cvrp}_{c} + \sum_{\substack{p\in N\\ p=v}} \sum_{e\in E} Y^{sp}_{p,e} \qquad \forall v\in N \qquad (37)$$

3.6. Power flow linear formulation

The installation of an EVCS at a transportation node leads to the energy consumption from the power distribution network, as long as the transportation node is an EVCS candidate (located on the same coordinates as the power distribution node). The operation of the electric network is assessed through the methodology shown in (Garces, 2016), which addresses a linear approximation of power flow on the complex plane. Nodal voltages and currents are represented through the admittance matrix Y (Grainger & Stevenson, 1994) of the electric network, expressed in Eq. (38).

$$\begin{bmatrix} I_{a,b,c}^{s} \\ I_{a,b,c}^{n} \end{bmatrix} = \begin{bmatrix} Y_{a,b,c}^{ss} & Y_{a,b,c}^{sn} \\ Y_{a,b,c}^{ns} & Y_{a,b,c}^{nn} \end{bmatrix} \begin{bmatrix} V_{a,b,c}^{s} \\ V_{a,b,c}^{n} \end{bmatrix} \tag{38}$$

where s is the slack node and n are the remaining nodes. Loads on the power distribution system are represented in (39) according to the *ZIP* model (Qian et al., 2011).

$$S = S_n \left(\frac{V_n}{V^{nom}} \right)^{\alpha} \tag{39}$$

The exponent α takes the value of 0, 1 or 2 for the constant power, current and impedance load respectively. If a Wye connected load is at node n, V^{nom} is the line to neutral voltage; otherwise it would be a line to line voltage for Delta-connected loads. Supported by the expression in Eq. (39), the voltage and current of a node can be associated in (40) as follows:

$$I_{a,b,c}^{n} = \frac{S_{n_{a,b,c}}^{p*}}{V_{a,b,c}^{n*}} + h \cdot S_{n_{a,b,c}}^{i*} + h^2 \cdot S_{n_{a,b,c}}^{z*} \cdot V_{a,b,c}^{n} \qquad h = \frac{1}{V^{nom}} \tag{40}$$

Being n any node other than the slack node; p, i, z, are the indices for the constant power, current and impedance load respectively. The *a,b,c* indices represent the three-phase system. Note that *ZIP* model is linear in $V_{a,b,c}^{n}$ except for the constant power loads. This term is approximated to obtain a linear power flow. A linear approximation is developed on the complex numbers (Flanigan, 1983) and not on the real set as in the conventional power flow formulations. The function $f(\Delta V) = 1/(1-\Delta V)$ is analytic for all $\|\Delta V\| < 1$. By using Taylor series around zero, the expression in Eq. (41) is obtained.

$$\frac{1}{1-\Delta V} = \sum_{n=0}^{\infty} (\Delta V)^n \qquad \|\Delta V\| < 1 \tag{41}$$

A linear form is shown in Eq. (42) by neglecting high order terms and defining $V = 1 - \Delta V$.

$$\frac{1}{V} = \frac{1}{1-\Delta V} \approx 1 + \Delta V = 2 - V \tag{42}$$

Note that Eq. (42) is valid for values of V close to 1 p.u. for example, the error for $V = 0.8$, this is, $\Delta V = 0.2$, is around 5% and decreases as V approaches to 1. Considering the Wye-connected loads, the first term of Eq. (40) is multiplied in the numerator and denominator by $T_{a,b,c} / V^{nom}$, where $T_{a,b,c} = [1 \; e^{-2\pi/3j} \; e^{2\pi/3j}]^T$. Then, this term becomes linear as presented in Eq. (43).

$$\frac{S_{n_{a,b,c}}^{p*}}{V_{a,b,c}^{n*}} = \frac{S_{n_{a,b,c}}^{p*}}{V_{a,b,c}^{n*}} \cdot \frac{1/\left(T_{a,b,c} / V^{nom}\right)}{1/\left(T_{a,b,c} / V^{nom}\right)} = h \cdot S_{n_{a,b,c}}^{p*} \circ \left(2 - h \cdot V_{a,b,c}^{n*} \circ T_{a,b,c}\right) \circ T_{a,b,c} \tag{43}$$

See that $(\cdot)$ is the conventional product and $(\circ)$ is the Hadamard product. In this manner, Eq. (40) is converted into Eq. (44):

$$I^n_{a,b,c} = 2h \cdot S^{p*}_{n_{a,b,c}} \circ T_{a,b,c} - h^2 \cdot S^{p*}_{n_{a,b,c}} \circ V^{n*}_{a,b,c} \circ T_{a,b,c}{}^2 + h \cdot S^{i*}_{n_{a,b,c}} + h^2 \cdot diag\left(S^{z*}_{n_{a,b,c}}\right) \cdot V^n_{a,b,c} \tag{44}$$

In Eq. (38) the expression for $I^n_{a,b,c}$ can be rewritten as follows:

$$I^n_{a,b,c} = Y^{ns}_{a,b,c} \cdot V^s_{a,b,c} + Y^{nn}_{a,b,c} \cdot V^n_{a,b,c} \tag{45}$$

Then, making equal Eq. (44) and Eq. (45), and after arranging some terms, Eq. (46), Eq.(47) and Eq. (48) are obtained:

$$A = Y^{ns}_{a,b,c} \cdot V^s_{a,b,c} - 2h \cdot S^{p*}_{n_{a,b,c}} \circ T_{a,b,c} - h \cdot S^{i*}_{n_{a,b,c}} \tag{46}$$

$$B = h^2 \cdot S^{p*}_{n_{a,b,c}} \circ T_{a,b,c}{}^2 \tag{47}$$

$$C = Y^{nn}_{a,b,c} - h^2 \cdot diag\left(S^{z*}_{n_{a,b,c}}\right) \tag{48}$$

Notice that the terms above are in accordance with $A + B \circ V^{n*}_{a,b,c} + C \cdot V^n_{a,b,c} = 0$. This latter requires to be solved in rectangular representation, as shown in (49), to obtain the nodal voltages.

$$\begin{bmatrix} -A_r \\ -A_i \end{bmatrix} = \begin{bmatrix} B_r + C_r & B_i - C_i \\ B_i + C_i & -B_r + C_r \end{bmatrix} \begin{bmatrix} V_r \\ V_i \end{bmatrix} \tag{49}$$

where r and i indicate real and imaginary part, respectively. It is necessary to clarify that the load drawn by EVs while charging, has to be added in the term $S^{i*}_{n_{a,b,c}}$, as this latter represents the constant current loads. The decision variable U_v, that determines the installation of an EVCS, is multiplied by P^{bat} (EV charging nominal power), and added to $S^{i*}_{n_{a,b,c}}$ in the power flow equations. In this sense, the term $S^{i*}_{n_{a,b,c}}$ is changed by $(S^{i*}_{n_{a,b,c}} + P^{bat} \cdot U_v)$ to include the impact of EVs charging on distribution network.

3.7. Objective function

The Eqs. (1-49) mentioned earlier represent the constraints of the proposed CSLP-EVFT problem. The objective function is comprised by the summation of six terms, shown in Eqs. (50-55), in which the installation and operation costs are involved.

$$C_1 = \left(365 \cdot \left(C^{travel} + C^{main}\right) \cdot \sum_{c \in N} \sum_{o \in N} \sum_{k \in K} x_{c,o,k} \cdot d_{c,o} \right) \cdot FA \tag{50}$$

$$C_2 = \left(365 \cdot \left(C^{travel} + C^{main}\right) \cdot \sum_{d \in N} \sum_{p \in N} \sum_{e \in E} y_{d,p,e} \cdot d_{d,p} \right) \cdot FA \tag{51}$$

Eqs. (50-51) are the costs associated with the routing performed by the EVs that follow the mobility patterns of CVRP and SP problem respectively. It is assumed that the routes are repeated daily along one year and the maintenance cost is also considered within the cost per kilometer traveled. The cost of EVCSs installation is depicted in Eq. (52), and the operation costs related with EVCSs energy consumption, are established in Eq. (53) and Eq. (54) for the CVRP and SP problem respectively. Notice that the time that an EV (either for CVRP or SP problem) takes to fully charge its battery is considered to be 0.5 hours (fast charging), assuming that this time will not affect the time to perform the routing.

$$C_3 = C^{const} \cdot \sum_{v \in N} U_v \tag{52}$$

$$C_4 = \left(365 \cdot 0.5 \cdot P^{bat} \cdot CE \cdot \sum_{c \in N} Y_c^{cvrp}\right) \cdot FA \tag{53}$$

$$C_5 = \left(365 \cdot 0.5 \cdot P^{bat} \cdot CE \cdot \sum_{p \in N} \sum_{e \in E} Y_{p,e}^{sp}\right) \cdot FA \tag{54}$$

Energy losses of the distribution system are computed in Eq. (55), based on the difference with respect to the benchmark case energy losses, e.g., without EVCSs. The term *Loss* is a non-linear expression that is deployed in Eq. (56) and Eq. (57).

$$C_6 = \left(365 \cdot 0.5 \cdot CE\right) \cdot \left(Loss - \overline{Loss}\right) \cdot FA \tag{55}$$

$$Loss = V_R^T G_{BUS} V_R + V_I^T G_{BUS} V_I \tag{56}$$

$$Loss = \begin{pmatrix} V_{RS} G_{SS} V_{RS} + V_{RS} G_{Sk} V_{Rk} + \\ V_{Rn} G_{nS} V_{RS} + V_{Rn} G_{nn} V_{Rn} + \\ V_{IS} G_{SS} V_{IS} + V_{IS} G_{Sn} V_{In} + \\ V_{In} G_{SS} V_{IS} + V_{In} G_{nn} V_{In} \end{pmatrix} \tag{57}$$

where G_{BUS} is the real part of admittance matrix and, V_R and V_I are the real and imaginary parts of nodal voltages, respectively. All of the costs except C_3, are affected by a factor of annualization *FA* to shift to present value the operation costs along the future years, which is computed according to (58). Notice that *nt* corresponds to the number of years in which the operation (routing, energy consumption and energy losses) is considered and *CPI* is the Consumer Price Index.

$$FA = \frac{nt}{\left(1 + CPI\right)^{nt}} \tag{58}$$

4. Test systems and CSLP-EVFT mathematical model validation

In order to validate the mathematical model proposed, two different test instances composed by combination of transportation networks and power distribution systems are proposed. Transportation and power networks are chosen from (Networking and Emerging Optimization, n.d.) and (IEEE Power and Energy Socierty, n.d.) respectively. The complete information related with the instances proposed in this work is presented in (Power Systems Planning Group, n.d.). The first system, shown in Fig. 1, is formed by the CVRP instance Pn19k2 and the 34-node distribution test system, which is named Pn19k2-IEEE34. Note that nodes joined with continuous line represent the power distribution system, being node 800 the distribution substation. Customers (drawn as solid squares) are identified by the numbers enclosed in squares, and electric nodes are in solid circles. Some nodes of the power network are made to coincide with the spatial location of all or part of the transportation network customers. These points are the candidate nodes for EVCSs.

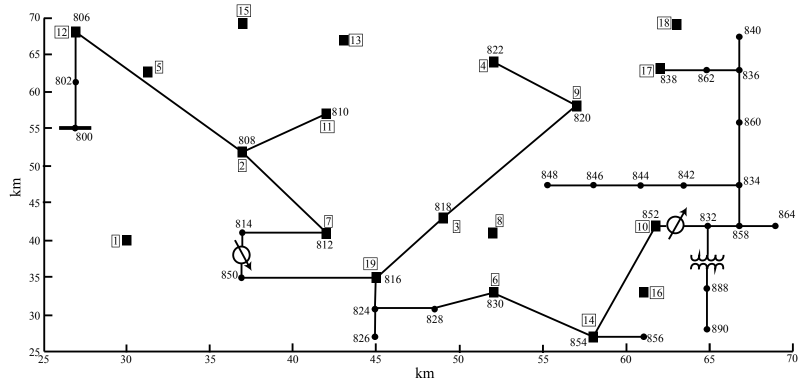

Fig. 1. Pn19k2-IEEE34 test system

A larger size test system is composed by the combination between the CVRP instance En22k4 and the 123-node distribution test system. The resulting test system is named En22k4-IEEE123 and shown in Figure. 2. Note that all the customers coincide with a node of the power network, except the depot node, which is identified with the number 1 enclosed in square. The distribution substation is located at node 150.

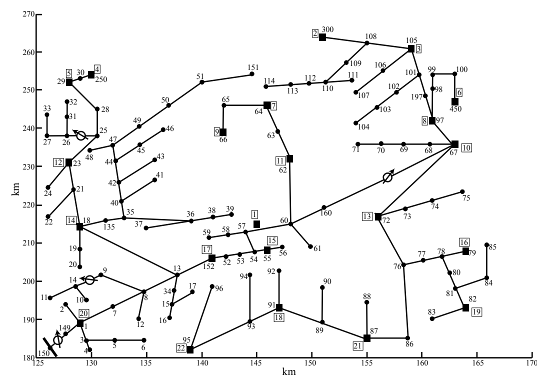

Fig. 2. En22k4-IEEE123 test system

CSLP-EVFT mathematical model validation is carried out by providing a large enough amount of EV battery autonomy Q^{cvrp} and Q^{sp}, in order to avoid the installation of EVCSs. In this sense the result for both transportation and power networks correspond to benchmark cases. Table 1 presents the objective function and the routes performed by the vehicles in each instance, considering only the transportation network.

Table 1
Benchmark case results with the transportation network approach

Instance	Objective function	Details of route	Time [S]
Pn19k2-IEEE34	212	1-7-9-17-18-4-13-15-12-5-1 1-19-6-14-16-10-8-3-11-2-1	416
En22k4-IEEE123	375	1-20-22-18-21-1 1-13-16-19-15-17-1 1-9-7-3-2-6-8-10-1 1-14-12-5-4-11-1	976

Since the point of view of the power distribution system, the voltages at electric nodes should be very close (and not the same as the power flow formulation corresponds to a linear one) to results reported on the IEEE database. Fig. 3 and Fig. 4 depict the difference in per unit of the voltages obtained with the CSLP-EVFT mathematical model, compared with the benchmark case voltages for Pn19k2-IEEE34 and En22k4-IEEE123 test systems respectively. The maximum difference in voltage is 1.3×10^{-3}.

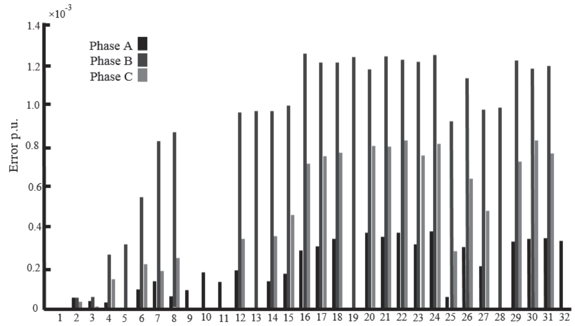

Fig. 3. Difference in voltage of Pn19k2-IEEE34 compared with benchmark case

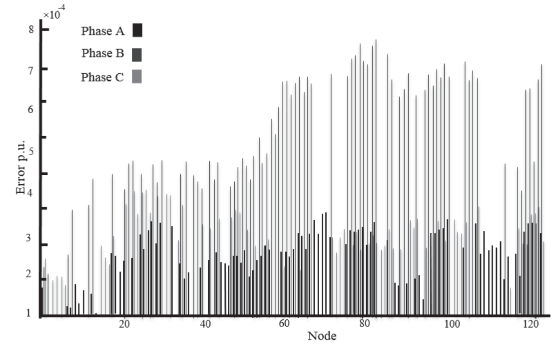

Fig. 4. Difference in voltage of En22k4-IEEE123 compared with benchmark case

The results shown above are based on the CSLP-EVFT mathematical model with the non-linear expression for the term $Loss$. In order to obtain a formulation that can be solved easily and with reduced computational times, the linearization of $Loss$ is proposed in (59) to (62). This procedure is carried out by using Taylor series around a point of operation, which is chosen as the operation of the power distribution system without EVCSs.

$$Loss = \Delta_{Loss} + Loss_{op} \tag{59}$$

$$\Delta_{Loss} = \begin{matrix} V_{RS}G_{Sn}\Delta V_{Rn} + \Delta V_{Rn}G_{nS}V_{RS} + \Delta V_{Rn}G_{nn}V_{Rno} + V_{Rno}G_{nn}\Delta V_{Rn} + \\ V_{IS}G_{Sn}\Delta V_{In} + \Delta V_{In}G_{nS}V_{IS} + \Delta V_{In}G_{nn}V_{Ino} + V_{Ino}G_{nn}\Delta V_{In} \end{matrix} \tag{60}$$

$$V_{Rn} = \Delta V_{Rn} + V_{Rno} \tag{61}$$

$$V_{In} = \Delta V_{In} + V_{Ino} \tag{62}$$

At the operation point power losses are identified as $Loss_{op}$, and real and imaginary parts of voltages at nodes (other than slack node *s*) are shown as V_{Rno} and V_{Ino} respectively.

5. Results

Coupled systems shown in Fig. 1 and Fig. 2, are utilized to assess the performance of CSLP-EVFT problem, considering the linear formulation presented for the term $Loss$. Parameters for Pn19k2-IEEE34 and En22k4-IEEE123 instances were chosen consistently to the reality. As reported by (Tesla Motors, 2017), an EVCS may draw up to 120 kW during 20 minutes from the electric distribution network for a 272 km battery range. In this work, the power demanded by the EV (for either the CVRP or SP problem) during the recharge is assumed to be 30 kW, as this value represents a suitable additional load for the distribution system and the duration of the recharge under this power would not affect the travel duration time. This value is introduced in the term $S^{i*}_{n_{a,b,c}}$ of the power flow equations, due to the recharge of the EVs can be represented as constant current load. The cost related with EVCS construction is 22000 USD, in accordance with (Agenbroad, 2014), considering type of installation, connectivity, materials, data and other factors. Since the point of view of the EVs operation, the average cost is 2.423 USD to travel 100 km, as reported by (U.S. Department of Energy, 2017), and an estimation of 100 USD is used under the concept of EV maintenance for every 5000 km traveled. The operation cost of the EVCSs, e.g., cost for both, energy consumed from the distribution network and energy losses, is estimated in 0.2 USD/kWh. Consumer Price Index *CPI* for the annualization factor is set to 10%. The proposed CSLP-EVFT model has been programmed and executed in the GAMS (General Algebraic Modeling System) environment (GAMS Development Corporation, 2016) on a HP desktop computer, Windows 64-bit operating system, with an Intel Core i3 @ 3.3 GHz processor and 4 GB of RAM. The non-linear approach (due to the non-linear expression for the term $Loss$) is solved using the DICOPT solver (GAMS Developmet Corporation, n.d.) and the linearized mathematical model is solved with CPLEX solver (GAMS

Development Corporation, n.d.). For all the cases, the limit time for run was 100000 seconds (almost 28 hours). Note that this is a long-term planning problem, and as such, the operation (EVs routing and energy consumption) shown in each solution, will not be affected by the computational times. These latter are depicted for reference.

5.1. *Pn19k2-IEEE34*

The results for instance *Pn19k2-IEEE34* are presented in Table 2, considering different values of battery autonomy, under the non-linearized approach of the mathematical model (non-linear expression for *Loss*). The first two columns show the values for autonomy Q^{cvrp} and Q^{sp} for CVRP and SP problems respectively. In the third column, the costs for each term at the objective function are presented. The routes sequence for each EV, following the respective mobility pattern (CVRP or SP), are shown in the sixth column. For all runs, the depot at CVRP is identified as "1" and the start and end points for the SP routes are the same. Numbers in bold are the EVCSs installed, which provide the recharge service for both type of EVs (CVRP and SP focuses). It is assumed that no more than one EV is able to be recharged at the same time.

Table 2
Results for Pn19k2-IEEE34 with non-linearized mathematical model

Q^{CVRP} [km]	Q^{SP} [km]	Costs [USD]	Mobility pattern	Detail of routes	Time [s]
30	20	C_1: 505872 C_2: 469413 C_3: 169400 C_4: 26042 C_5: 22787 C_6: 3985	CVRP	1-11-**2**-8-**10**-16-14-**6**-19-7-1 1-**3**-**9**-17-18-**4**-13-15-**12**-5-1	1238
			SP	12-5-**2**-7-**3**-8-10 1-**2**-11-**4**-18 15-**2**-7-**3**-8-6-14 17-9-**4**-11-**2**-5-12	
40	24	C_1: 530938 C_2: 437511 C_3: 121000 C_4: 19531 C_5: 16276 C_6: 2494	CVRP	1-**11**-13-4-18-**17**-9-10-16-**14**-6-1 1-2-5-**12**-15-**3**-8-19-7-1	2870
			SP	12-15-**11**-**3**-8-10 1-2-**11**-4-18 15-**11**-**3**-8-6-14 17-9-**11**-15-12	
50	28	C_1: 483085 C_2: 426118 C_3: 121000 C_4: 16276 C_5: 13021 C_6: 2125	CVRP	1-**19**-6-14-16-10-8-**3**-11-2-1 1-7-**9**-17-18-4-13-15-**12**-5-1	1779
			SP	12-15-**11**-10 1-2-**11**-4-18 15-**11**-**3**-8-6-14 17-9-**11**-15-12	
60	32	C_1: 483085 C_2: 426118 C_3: 72600 C_4: 16276 C_5: 6510 C_6: 1772	CVRP	1-19-6-14-16-**10**-8-3-11-2-1 1-7-9-17-18-**4**-13-15-12-5-1	1541
			SP	12-15-**11**-10 1-2-**11**-4-18 15-**11**-**10**-16-14 17-9-**4**-13-15-12	
70	36	C_1: 508151 C_2: 414724 C_3: 48400 C_4: 13021 C_5: 6510 C_6: 901	CVRP	1-7-8-3-**11**-13-15-12-5-2-1 1-19-6-14-16-10-**9**-17-18-4-1	1163
			SP	12-15-**11**-10 1-2-**11**-4-18 15-**11**-3-8-6-14 17-**9**-4-13-15-12	
80	40	C_1: 483085 C_2: 414724 C_3: 48400 C_4: 9765 C_5: 6510 C_6: 901	CVRP	1-7-**9**-17-18-4-13-15-12-5-1 1-19-6-14-16-10-8-3-**11**-2-1	411
			SP	12-15-**11**-10 1-2-**11**-4-18 15-**11**-3-8-6-14 17-9-4-13-15-12	
			SP	12-15-11-10 1-2-11-4-18 15-11-3-8-6-14 17-9-4-13-15-12	
90	44	C_1: 483085 C_2: 414724 C_3: 48400 C_4: 9765 C_5: 6510 C_6: 184	CVRP	1-2-**11**-3-8-10-16-14-6-19-1 1-7-9-17-18-4-13-15-**12**-5-1	870
			SP	12-15-**11**-10 1-2-**11**-4-18 15-**11**-3-8-6-14 17-9-4-13-15-12	
100	48	C_1: 483085 C_2: 430675 C_3: 24200 C_4: 3255 C_5: 3255 C_6: 757	CVRP	1-7-9-17-18-**4**-13-15-12-5-1 1-19-6-14-16-10-8-3-11-2-1	117
			SP	12-15-11-10 1-2-11-4-18 15-13-**4**-9-10-16-14 17-9-4-13-15-12	
110	52	C_1: 496760 C_2: 414720 C_3: 24200 C_4: 0 C_5: 3255 C_6: 19	CVRP	1-7-9-17-18-4-13-15-**12**-5-1 1-19-6-14-16-10-8-3-2-11-1	242
			SP	12-15-11-10 1-2-11-4-18 15-11-3-8-6-14 17-9-4-13-15-12	
120	56	C_1: 483085 C_2: 414724 C_3: 0 C_4: 0 C_5: 0 C_6: 0	CVRP	1-19-6-14-16-10-8-3-11-2-1 1-7-9-17-18-4-13-15-12-5-1	500
			SP	12-15-11-10 1-2-11-4-18 15-11-3-8-6-14 17-9-4-13-15-12	
130	60	C_1: 483085 C_2: 414724 C_3: 0 C_4: 0 C_5: 0 C_6: 0	CVRP	1-2-11-3-8-10-16-14-6-19-1 1-5-12-15-13-4-18-17-9-7-1	425
			SP	12-15-11-10 1-2-11-4-18 15-11-3-8-6-14 17-9-4-13-15-12	

According to Table 2, as the battery autonomy is increased, there is a reduction of costs associated with EVCS installation (C_3) and energy consumption (C_4 and C_5). Notice that cost of delta of energy losses in C_6 is also decreased. Although this, the routing cost shown in C_1 and C_2 may not necessarily decrease with the increment of the battery autonomy, as the candidate points for EVCS coincide with the customers location, otherwise, a change in these costs would be noticeable. The last two runs only depict costs for EVs routing, being these cases the representation of the benchmark case results, as no EVCSs are installed and therefore the energy consumption and delta of losses are null.

In Table 3, the results for Pn19k2-IEEE34 are shown, under the context of the linearized mathematical model, considering the linear expression for the term *Loss*. This aspect makes the problem to be solved in less computational times compared with the non-linearized model. Besides of this, there is a reduction in the overall cost of the objective function, on behalf of the costs for CVRP and SP routing and delta of energy losses. This latter is strongly related with the EVCSs location, which are attempted to be installed as close as to the distribution substation or at three-phase nodes. The EVCSs installation at one-phase electric nodes may provide larger power losses in comparison to three-phase nodes.

Table 3
Results for Pn19k2-IEEE34 with linearized mathematical model

Q^{CVRP} [km]	Q^{SP} [km]	Costs [USD]	Mobility pattern	Detail of routs	Time [s]
30	20	C_1: 489921 C_2: 442069 C_3: 193600 C_4: 29297 C_5: 22787 C_6: 2417	CVRP	1-7-19-**6**-14-16-**10**-8-**11**-2-1 1-5-**12**-15-13-**4**-18-17-**9**-**3**-1	451
			SP	12-5-**2**-7-**3**-8-10 1-**2**-11-**4**-18 15-**11**-**3**-8-6-14 17-**9**-**11**-2-5-12	
40	24	C_1: 483085 C_2: 437511 C_3: 145200 C_4: 19531 C_5: 16276 C_6: 1448	CVRP	1-7-**9**-17-18-**4**-13-15-**12**-5-1 1-19-6-**14**-16-10-8-**3**-11-2-1	399
			SP	12-15-**11**-**3**-8-10 1-2-**11**-4-18 15-11-**3**-8-6-14 17-9-**11**-15-12	
50	28	C_1: 483085 C_2: 426118 C_3: 121000 C_4: 16276 C_5: 13021 C_6: 1015	CVRP	1-7-**9**-17-18-4-13-15-**12**-5-1 1-**19**-6-14-16-10-8-**3**-11-2-1	624
			SP	12-15-**11**-10 1-2-**11**-4-18 15-**11**-**3**-8-6-14 17-9-**11**-15-12	
60	32	C_1: 483085 C_2: 414724 C_3: 96800 C_4: 13021 C_5: 6510 C_6: 1368	CVRP	1-5-12-15-13-**4**-18-17-9-7-1 1-2-11-3-8-**10**-16-14-6-19-1	95
			SP	12-15-**11**-10 1-2-**11**-4-18 15-11-**3**-8-6-14 17-9-**4**-13-15-12	
70	36	C_1: 483085 C_2: 414724 C_3: 72600 C_4: 13021 C_5: 6510 C_6: 522	CVRP	1-5-12-15-13-**4**-18-17-9-7-1 1-2-11-**3**-8-10-16-14-6-19-1	188
			SP	12-15-**11**-10 1-2-**11**-4-18 15-**11**-3-8-6-14 17-9-**4**-13-15-12	
80	40	C_1: 483085 C_2: 414724 C_3: 48400 C_4: 9765 C_5: 6510 C_6: 299	CVRP	1-5-12-15-13-**4**-18-17-9-7-1 1-19-6-14-16-10-8-3-**11**-2-1	287
			SP	12-15-**11**-10 1-2-**11**-4-18 15-**11**-3-8-6-14 17-9-4-13-15-12	
90	44	C_1: 483085 C_2: 414724 C_3: 48400 C_4: 9765 C_5: 6510 C_6: 293	CVRP	1-7-**9**-17-18-4-13-15-12-5-1 1-19-6-14-16-10-8-3-**11**-2-1	141
			SP	12-15-**11**-10 1-2-**11**-4-18 15-**11**-3-8-6-14 17-9-4-13-15-12	
100	48	C_1: 483085 C_2: 430675 C_3: 24200 C_4: 3255 C_5: 3255 C_6: 239	CVRP	1-5-12-15-13-4-18-17-**9**-7-1 1-2-11-3-8-10-16-14-6-19-1	163
			SP	12-15-11-10 1-2-11-4-18 15-13-4-**9**-10-16-14 17-9-4-13-15-12	
110	52	C_1: 483085 C_2: 414724 C_3: 24200 C_4: 0 C_5: 3255 C_6: 19	CVRP	1-5-**12**-15-13-4-18-17-9-7-1 1-19-6-14-16-10-8-3-11-2-1	332
			SP	12-15-11-10 1-2-11-4-18 15-11-3-8-6-14 17-9-4-13-15-12	
120	56	C_1: 483085 C_2: 414724 C_3: 0 C_4: 0 C_5: 0 C_6: 0	CVRP	1-5-12-15-13-4-18-17-9-7-1 1-2-11-3-8-10-16-14-6-19-1	177
			SP	12-15-11-10 1-2-11-4-18 15-11-3-8-6-14 17-9-4-13-15-12	
130	60	C_1: 483085 C_2: 414724 C_3: 0 C_4: 0 C_5: 0 C_6: 0	CVRP	1-7-9-17-18-4-13-15-12-5-1 1-2-11-3-8-10-16-14-6-19-1	286
			SP	12-15-11-10 1-2-11-4-18 15-11-3-8-6-14 17-9-4-13-15-12	

5.2. En22k4-IEEE123

The increment in customers and electric nodes on transportation and power distribution networks respectively, contributes to increase computational effort for finding a solution, which can be seen in Table 4 for instance En22k4-IEEE123. As the battery autonomy is increased, the installation of EVCSs is less required and hence the energy drawn by EVs from the distribution system is reduced, as noted in C_3, C_4 and C_5. Cost associated with delta of energy losses also follows a descending behavior to reach a point, in which no EVCSs must be installed, e.g., the objective function is only affected by the routing costs established in C_1 and C_2 for CVRP and SP approaches respectively.

As performed with the first instance, runs with the linearized mathematical model are also implemented. In Table 5 the runs for different values of battery autonomy are shown. Under the linearized approach, the majority of the executions present a reduced cost of CVRP and SP routing, and EVCSs installation. The latter does not apply to the first case ($Q^{CVRP}=30\ km$ and $Q^{SP}=30\ km$) in which the EVCS installation cost is greater compared with the non-linearized model. Notice in Table 5 that the EVCS installed at customer 17 serves the EVs associated with SP problem, in contrast with the non-linearized case where the same EVCS serves both type of EVs. In regards with delta of energy losses, it is supposed that this cost should be reduced as the battery autonomy increases. However, this cost is increased in some cases, i.e., when the autonomy changes from Q^{CVRP}=120 *km* and Q^{SP}=75 *km* to Q^{CVRP}=150 *km* and Q^{SP}=80 *km*. Although the number of EVCSs installed is the same for both cases, the cost of energy losses is greater in the second case (Q^{CVRP}=150 *km* and Q^{SP}=80 *km*), because the electrical path from the distribution substation to the EVCS installed at customer 14 is less than that for the customer at 9 (See Figure 2). Since the point of view of the computational effort, the run times for most of the cases decrease notably in comparison to results shown in Table 4.

Table 4
Results for En22k4-IEEE123 with non-linearized mathematical model

Q^{CVRP} [km]	Q^{SP} [km]	Costs [USD]	Mobility pattern	Detail of routes	Time [s]
30	30	C_1: 881860 C_2: 619810 C_3: 338800 C_4: 26042 C_5: 45574 C_6: 2333	CVRP	1-12-5-4-2-3-7-9-1 1-15-18-22-21-19-16-1 1-13-8-6-10-11 1-17-20-14-1	24793
			SP	5-4-9-11-13-16-19 12-9-11-13-16 14-9-11-8-10 20-17-1-11-8-6-3	
40	35	C_1: 890970 C_2: 617530 C_3: 266200 C_4: 22787 C_5: 32553 C_6: 1694	CVRP	1-15-22-20-17-1 1-16-19-21-18-13-1 1-10-8-6-3-2-11-1 1-14-12-5-4-7-9-1	16433
			SP	5-4-9-11-13-16-19 12-14-17-15-16 14-9-11-8-10 20-17-1-11-8-3	
50	40	C_1: 863630 C_2: 617530 C_3: 217800 C_4: 19532 C_5: 19532 C_6: 1348	CVRP	1-15-17-22-20-1 1-7-2-3-6-8-10-1 1-13-16-19-21-18-1 1-14-12-4-5-9-11-1	9304
			SP	5-4-9-11-13-16-19 12-9-11-13-16 14-9-11-8-10 20-17-1-11-8-3	
60	45	C_1: 893250 C_2: 633480 C_3: 145200 C_4: 16276 C_5: 13021 C_6: 927	CVRP	1-10-8-6-3-2-1 1-11-9-7-5-4-12-14-1 1-17-15-22-20-1 1-13-16-19-21-18-1	3128
			SP	5-4-9-11-13-16-19 12-9-11-13-16 14-17-1-11-8-10 20-17-1-13-8-3	
70	50	C_1: 856790 C_2: 617530 C_3: 145200 C_4: 13021 C_5: 13021 C_6: 1038	CVRP	1-11-4-5-12-14-1 1-13-16-19-21-18-1 1-10-8-6-3-2-7-9-1 1-15-22-20-17-1	3209
			SP	5-4-9-11-13-16-19 12-14-17-15-16 14-9-11-8-10 20-17-1-11-8-3	
80	55	C_1: 888700 C_2: 617530 C_3: 72600 C_4: 9765 C_5: 6510 C_6: 580	CVRP	1-20-14-17-1 1-9-7-3-2-4-5-12-1 1-11-6-8-10-13-1 1-16-19-21-22-18-15-1	1526
			SP	5-4-9-11-13-16-19 12-14-17-15-16 14-9-11-8-10 20-17-1-11-8-3	
90	60	C_1: 900090 C_2: 617530 C_3: 48400 C_4: 6510 C_5: 3255 C_6: 370	CVRP	1-9-7-3-2-4-5-12-1 1-14-20-22-18-1 1-10-8-6-11-13-1 1-17-15-21-19-16-1	1313
			SP	5-4-9-11-13-16-19 12-14-17-15-16 14-9-11-8-10 20-17-1-11-8-3	
100	65	C_1: 916040 C_2: 617530 C_3: 48400 C_4: 6510 C_5: 6510 C_6: 364	CVRP	1-15-17-21-19-16-1 1-14-20-22-18-1 1-11-8-6-3-2-7-9-1 1-13-10-4-5-12-1	2377
			SP	5-4-9-11-13-16-19 12-9-11-13-16 14-9-11-8-10 20-17-1-11-8-3	
110	70	C_1: 900090 C_2: 617530 C_3: 48400 C_4: 6510 C_5: 3255 C_6: 371	CVRP	1-13-16-19-21-18-1 1-17-15-20-22-1 1-3-2-6-8-10-1 1-14-12-5-4-7-9-11-1	1361
			SP	5-4-9-11-13-16-19 12-9-11-13-16 14-9-11-8-10 20-17-1-11-8-3	
120	75	C_1: 881860 C_2: 631200 C_3: 24200 C_4: 3255 C_5: 0 C_6: 110	CVRP	1-10-8-6-3-2-7-1 1-14-20-22-18-15-1 1-12-5-4-9-11-13-1 1-17-21-19-16-1	956
			SP	5-4-9-11-13-16-19 12-14-17-15-16 14-9-11-8-10 20-14-9-7-2-3	
150	80	C_1: 881860 C_2: 631200 C_3: 24200 C_4: 3255 C_5: 0 C_6: 196	CVRP	1-13-16-19-21-18-1 1-11-2-3-6-8-10-1 1-14-12-5-4-7-9-1 1-20-22-15-17-1	1690
			SP	5-4-9-11-13-16-19 12-14-17-15-16 14-9-11-8-10 20-14-9-7-2-3	
200	130	C_1: 854520 C_2: 617530 C_3: 0 C_4: 0 C_5: 0 C_6: 0	CVRP	1-7-2-3-6-8-10-1 1-14-12-5-4-9-11-1 1-13-16-19-21-18-1 1-15-22-20-17-1	976
			SP	5-4-9-11-13-16-19 12-14-17-15-16 14-9-11-8-10 20-17-1-11-8-3	

Table 5
Results for En22k4-IEEE123 with linearized mathematical model

Q^{CVRP} [km]	Q^{SP} [km]	Costs [USD]	Mobility pattern	Detail of routes	Time [s]
30	30	C_1: 856790 C_2: 617530 C_3: 363000 C_4: 26042 C_5: 48829 C_6: 2477	CVRP	1-9-7-2-3-6-8-10-1 1-14-12-5-4-11-1 1-18-21-19-16-13-1 1-15-22-20-17-1	3460
			SP	5-4-9-11-13-16-19 12-9-11-13-16 14-9-11-8-10 20-17-1-11-8-3	
40	35	C_1: 856790 C_2: 622090 C_3: 242000 C_4: 19532 C_5: 32553 C_6: 1593	CVRP	1-9-7-2-3-6-8-10-1 1-14-12-5-4-11-1 1-17-20-22-15-1 1-13-16-19-21-18-1	698
			SP	5-4-9-11-13-16-19 12-9-11-13-16 14-9-11-8-10 20-17-15-1-11-8-3	
50	40	C_1: 888700 C_2: 631200 C_3: 193600 C_4: 19532	CVRP	1-10-8-6-3-2-11-1 1-13-16-19-21-22-1 1-17-20-18-15-1 1-14-12-5-4-7-9-1	2994
90	60	C_1: 854520 C_2: 617530 C_3: 48400 C_4: 6510 C_5: 6510 C_6: 367	CVRP	1-15-22-20-17-1 1-18-21-19-16-13-1 1-10-8-6-3-2-7-1 1-14-12-5-4-9-11-1	376
			SP	5-4-9-11-13-16-19 12-9-11-13-16 14-9-11-8-10 20-17-1-11-8-3	
100	65	C_1: 861350 C_2: 617530 C_3: 48400 C_4: 6510 C_5: 6510 C_6: 375	CVRP	1-15-22-20-17-1 1-13-16-19-21-18-1 1-9-7-2-3-6-8-10-1 1-11-5-4-12-14-1	144
			SP	5-4-9-11-13-16-19 12-9-11-13-16 14-9-11-8-10 20-17-1-11-8-3	
110	70	C_1: 868190 C_2: 617530 C_3: 24200 C_4: 6510	CVRP	1-11-2-3-6-8-10-1 1-14-12-5-4-7-9-1 1-15-17-20-22-1 1-13-16-19-21-18-1	1056

		C_5: 19532 C_6: 1265	SP	5-4-**9**-11-**13**-16-19 12-**14**-17-15-16 14-**9**-11-8-10 20-**14**-**9**-7-2-3	
60	45	C_1: 872740 C_2: 617530 C_3: 145200 C_4: 16276 C_5: 16276 C_6: 999	CVRP	1-7-2-**3**-6-8-10-1 1-20-**22**-21-18-1 1-**11**-9-4-5-**12**-14-1 1-17-15-19-**16**-13-1	71
			SP	5-4-9-**11**-13-16-19 12-9-**11**-13-16 14-9-**11**-8-10 20-**17**-1-**11**-8-3	
70	50	C_1: 925150 C_2: 617530 C_3: 121000 C_4: 13021 C_5: 13021 C_6: 729	CVRP	1-7-2-**3**-6-8-10-1 1-16-19-**21**-22-18-15-1 1-17-**20**-14-1 1-13-4-**5**-12-9-11-1	3189
			SP	5-4-9-**11**-13-16-19 12-9-**11**-13-16 14-9-**11**-8-10 20-17-1-**11**-8-3	
80	55	C_1: 854520 C_2: 617530 C_3: 96800 C_4: 9765 C_5: 9765 C_6: 767	CVRP	1-7-2-3-6-**8**-10-1 1-15-22-20-17-1 1-14-12-5-4-**9**-11-1 1-18-21-19-16-**13**-1	990
			SP	5-4-9-**11**-13-16-19 12-14-17-15-16 14-9-**11**-8-10 20-17-1-**11**-8-3	
		C_5: 3255 C_6: 176	SP	5-4-9-**11**-13-16-19 12-9-11-13-16 14-9-11-8-10 20-17-1-**11**-8-3	
120	75	C_1: 909200 C_2: 617530 C_3: 24200 C_4: 3255 C_5: 0 C_6: 176	CVRP	1-14-12-5-4-7-9-1 1-13-20-17-1 1-10-8-6-3-2-11-1 1-16-19-21-22-18-15-1	2002
			SP	5-4-9-11-1316-19 12-14-17-15-16 14-9-11-8-10 20-17-1-**11**-8-3	
150	80	C_1: 854520 C_2: 617530 C_3: 24200 C_4: 3255 C_5: 0 C_6: 90	CVRP	1-10-8-6-3-2-7-1 1-11-9-4-5-12-14-1 1-17-20-22-15-1 1-18-21-19-16-13-1	1113
			SP	5-4-9-11-13-16-19 12-9-11-13-16 14-9-11-8-10 20-**17**-1-11-8-3	
200	130	C_1: 854520 C_2: 617530 C_3: 0 C_4: 0 C_5: 0 C_6: 0	CVRP	1-18-21-19-16-13-1 1-7-2-3-6-8-10-1 1-11-9-4-5-12-14-1 1-17-20-22-15-1	46
			SP	5-4-9-11-13-16-19 12-9-11-13-16 14-9-11-8-10 20-17-1-11-8-3	

For the run with Q^{CVRP}=90 and Q^{SP}=60, in Tables 4 and 5 for the non-linear and linearized mathematical models respectively, two EVCSs are required to perform the respective routings. In the non-linearized model, two EVCSs are installed at nodes 3 and 11, whilst in the linearized model the nodes 8 and 11 are chosen as solution to install EVCSs. If this is revised in detail in Figure 2, the electrical path from the substation to node 3 is longer than that presented for node 8, which results in a reduction of the energy losses cost (See value C_6) in the linearized model.

On the other hand, specifically for the linearized model, it is necessary to examine some of the cases in Table 5, as the results are not obvious in the context of energy losses. Not always the larger the battery capacity, the less the costs implied in the energy losses (C_6). For the runs Q^{CVRP}=70 - Q^{SP}=50 (case 1) and Q^{CVRP}=80 - Q^{SP}=55 (case 2), the cost C_6 is 729 and 767, and the number of EVCSs are 5 and 4 respectively. Notice that in this comparison, although the number of EVCSs installed is reduced with the increment of battery capacity, the energy losses are decreased. This is due to that the voltage profile of the electric nodes in the case 1 is better than that presented for case 2. Energy losses are dependent on the voltage at distribution nodes as depicted in (56), and as such, incur in the operation point of the system. See in Fig. 5 the voltage difference between case 1 and case 2, showing a negative difference in the majority of the nodes, which accounts for a better voltage profile for case 1. Accordingly, the energy losses for case 1 are less than those for case 2, as presented in Table 5.

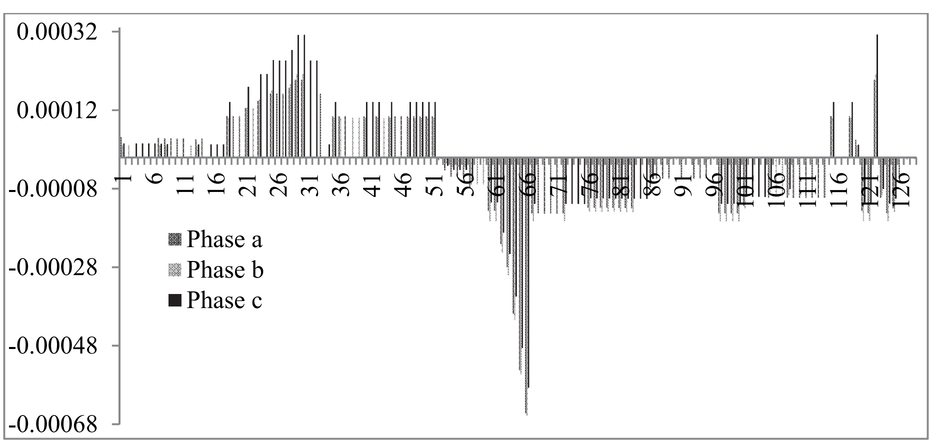

Fig. 5. Voltage difference between runs Q^{CVRP}=70 - Q^{SP}=50 and Q^{CVRP}=80 - Q^{SP}=55

In order to assess the linearized model in terms of the power flow formulation, the maximum voltage difference respect to the non-linearized model (non-linear term for $Loss$) is found in Table 6 for both instances.

Table 6
Maximum voltage difference between non-linearized and linearized models

Pn19k2-IEEE34			En22k4-IEEE123		
Q^{CVRP} [km]	Q^{SP} [km]	Max. Dif. [p.u]	Q^{CVRP} [km]	Q^{SP} [km]	Max. Dif. [p.u]
30	20	0.016366226	30	30	0.000402307
40	24	0.010846248	40	35	0.000276445
50	28	0.010447972	50	40	0.0003341
60	32	0.006739884	60	45	0.000331383
70	36	0.003773189	70	50	0.000753311
80	40	0.005995303	80	55	0.000879476
90	44	0.002535781	90	60	6.82391E-05
100	48	0.006798513	100	65	6.82391E-05
110	52	0.00358965	110	70	0.000589611
120	56	7.96501E-11	150	80	0.000715173
130	60	7.96501E-11	200	130	2.6835E-10

According to Table 6, as the battery autonomy is reduced, the voltage difference between two models is increased, because the installation of EVCSs makes the power distribution point of operation to move away from the point over which the linearization was carried out (without EVCSs installed). Notice that this linearization shown better results for En22k4-IEEE123 instance, due to the robustness of this distribution system to meet more loads, compared with results of Pn19k2-IEEE34 instance. As demonstrated above, the energy losses are not only impacted by how close or how far the EVCSs are from the power source, but also by the type of node (one-phase or three-phase) in which the EVCS is installed. In some cases, the resulting location of an EVCS is at a three-phase node, although this action requires an increase in the routing cost. However, this situation is sometimes more cost-effective for the objective function, as the energy losses cost are less, compared with that when the EVCS is installed at a one-phase node that is closer to the substation.

Furthermore, the linearized model can reduce the energy losses, no matter that in some cases the number of EVCSs installed was increased compared with the non-linearized model. This is due to the fact that the linearized model can obtain an operation point of the distribution system with a better voltage profile, which impacts directly the energy losses (see Equation (56) for reference). In the same manner, other costs are reduced, such as routing for CVRP and SP, significantly affecting the overall cost of the objective function.

6. Conclusions

Many companies have had facility location and vehicle routing as two of the most crucial decisions to reduce logistics cost. For a logistics corporation, equipped with a fleet of electric vehicles, the routing cost is directly affected by the location strategy for charging stations. On the other hand, this aspect leads to impact the power distribution network, since the point of view of the electric utility. Therefore, this paper studied the Charging Station Location Problem of Electric Vehicles for Freight Transportation CSLP-EVFT to improve the performance of transportation network and power distribution system.

The distance traveled by the EVs, introduced along the mathematical model, represented an appropriate alternative to optimally locate Electric Vehicle Charging Stations EVCSs on the transportation network with the equivalent nodes on the distribution system. By the other side, the battery autonomy is considered as a critical factor in the EVCSs location, as this is described in terms of the distance that can be traveled. When no EVCSs were installed, as a consequence of too large battery autonomy, the linear formulation of power flow, depicted in the mathematical model, had reasonable results compared with benchmark case results, showing a maximum difference of $1.3x10^{-3}$ p.u. Due to the presence of a non-linear expression for the term *Loss* in the objective function, a Taylor series based linearization was used to obtain a mathematical model completely linearized. This focus leads not only to handle this nonlinearity, but also reduce the overall objective function, which involves the cost of EVs routing, installation and energy consumption of EVCSs, and delta of energy losses. In many cases, the computational times of runs was improved notably. For any case, the non-linearized or linearized mathematical model, the EVCSs location involves a change in the term for delta of energy losses. This term is reduced whether by means the EVCS is installed as close as to the distribution substation or at a one-phase or three-phase distribution node. In regards with the power distribution system operation, the voltage difference between the linearized and non-linearized mathematical models is increased as the battery autonomy is reduced. This is because the installation of EVCSs makes the power distribution point of operation to move away from the point over which the linearization was carried out (without EVCSs installed). The robustness of the distribution system incurs in the results shown by the linearization. The mathematical model addressed in this work, suggests a unique owner of the transportation company and the distribution system, including the charging stations. Otherwise, the problem should be handled considering a bi-level approach, being the routing solution and EVCSs location, the input to find the energy consumption and energy losses with the power flow formulation.

7. Future Works

As part of the future research, the introduction of the index *t* in several parameters and variables will be considered, e.g. number of customers and fleet size could increase over the course of the time. The use of stronger methodologies and solution techniques, such as meta-heuristics and set partitioning will be taken into account for larger instances, reflecting a more realistic situation of the mathematical model proposed. By the other side, a better alternative for the transportation problem may be the multi-depot vehicle routing problem, as this corresponds to one of the expansion strategies of the freight transportation companies. From the perspective of the power flow equations, these may be treated in polar coordinates, so that the maximum and minimum voltage node can be introduced.

References

Abapour, S., Abapour, M., Khalkhali, K., & Moghaddas-Tafreshi, S. M. (2015). Application of data envelopment analysis theorem in plug-in hybrid electric vehicle charging station planning. *IET Generation, Transmission & Distribution*, *9*(7), 666–676.

Agenbroad, J. (2014). Pulling Back the Veil on EV Charging Station Costs - Rocky Mountain Institute. Retrieved June 1, 2017, from https://www.rmi.org/news/pulling-back-veil-ev-charging-station-costs/

Aghaebrahimi, M. R., Ghasemipour, M. M., & Sedghi, A. (2014). Probabilistic optimal placement of EV parking considering different operation strategies. In *MELECON 2014 - 2014 17th IEEE Mediterranean Electrotechnical Conference* (pp. 108–114). IEEE.

Arias, A., Granada, M., & Castro, C. A. (2017). Optimal probabilistic charging of electric vehicles in distribution systems. *IET Electrical Systems in Transportation*, *7*(3), 246–251.

Arias, A., Sanchez, J. D., & Granada, M. (2017). Integrated planning of electric vehicles routing and charging stations location considering transportation networks and power distribution systems.

Carradore, L., & Turri, R. (2011). Electric Vehicles participation in distribution network voltage regulation (p. 6). Cardiff, Wales, UK: [Institution of Engineering and Technology].

Clement-Nyns, K., Haesen, E., & Driesen, J. (2010). The Impact of Charging Plug-In Hybrid Electric Vehicles on a Residential Distribution Grid. *IEEE Transactions on Power Systems*, *25*(1), 371–380.

Cui, S., Ai, X., Dong, R., Liang, W., & Dong, C. (2014, August). Electric vehicle charging station planning based on sensitivity analysis. In *2014 IEEE Conference and Expo Transportation Electrification Asia-Pacific (ITEC Asia-Pacific)*(pp. 1-5). IEEE.

del Razo, V., & Jacobsen, H.-A. (2016). Smart Charging Schedules for Highway Travel With Electric Vehicles. *IEEE Transactions on Transportation Electrification*, *2*(2), 160–173.

Feng, L., Ge, S., & Liu, H. (2012a). Electric Vehicle Charging Station Planning Based on Weighted Voronoi Diagram. In *2012 Asia-Pacific Power and Energy Engineering Conference* (pp. 1–5). IEEE.

Feng, L., Ge, S., Liu, H., Wang, L., & Feng, Y. (2012b). The planning of charging stations on the urban trunk road. In *IEEE PES Innovative Smart Grid Technologies* (pp. 1-4). IEEE.

Flanigan, F. J. (1983). *Complex variables : harmonic and analytic functions*. Dover Publications. Retrieved from https://books.google.es/books?hl=en&lr=&id=nGugK5grZPgC&oi=fnd&pg=PP1&dq=F.+Flanigan,

+Complex+Variables&ots=rsWLiLQjuV&sig=q6_5AAtvq7T1qA3OlU36nkBe1Cg#v=onepage&q=F. Flanigan%2C Complex Variables&f=false

GAMS Development Corporation. (n.d.). CPLEX 12 solver. Retrieved December 6, 2017, from https://www.gams.com/latest/docs/S_CPLEX.html

GAMS Development Corporation. (2016). GAMS Solvers. Retrieved June 1, 2017, from https://gams.com/latest/docs/solvers/index.html

GAMS Developmet Corporation. (n.d.). DICOPT solver. Retrieved December 6, 2017, from https://www.gams.com/24.8/docs/solvers/dicopt/index.html

Garces, A. (2016). A Linear Three-Phase Load Flow for Power Distribution Systems. *IEEE Transactions on Power Systems*, *31*(1), 827–828.

Grainger, J., & Stevenson, W. (1994). Power system analysis. Retrieved from https://www.uvic.ca/engineering/ece/assets/docs/current/undergraduate/201801/ELEC488.pdf

Hu, Z., & Song, Y. (2012). Distribution network expansion planning with optimal siting and sizing of electric vehicle charging stations. In *2012 47th International Universities Power Engineering Conference (UPEC)* (pp. 1–6). IEEE.

IEEE Power and Energy Socierty. (n.d.). Distribution Test Feeders - Distribution Test Feeder Working Group - IEEE PES Distribution System Analysis Subcommittee. Retrieved December 6, 2017, from http://www.ewh.ieee.org/soc/pes/dsacom/testfeeders/index.html

Ip, A., Fong, S., (IMS), E. L.-M. and S., 6th, 2010, & 2010, undefined. (n.d.). Optimization for allocating BEV recharging stations in urban areas by using hierarchical clustering. *Ieeexplore.ieee.org*. Retrieved from http://ieeexplore.ieee.org/abstract/document/5713494/

Jia, L., Hu, Z., Song, Y., & Luo, Z. (2012). Optimal siting and sizing of electric vehicle charging stations. In *2012 IEEE International Electric Vehicle Conference* (pp. 1–6). IEEE.

Liu, Z., Wen, F., & Ledwich, G. (2013). Optimal Planning of Electric-Vehicle Charging Stations in Distribution Systems. *IEEE Transactions on Power Delivery*, *28*(1), 102–110.

Liu, Z., Zhang, W., Ji, X., & Li, K. (2012). Optimal Planning of charging station for electric vehicle based on particle swarm optimization. In *IEEE PES Innovative Smart Grid Technologies* (pp. 1–5).

Luo, H., Ruan, J., & Li, F. (2011). Study on the Electric Vehicles Ownership and Planning for the Construction of Charging Infrastructure. In *2011 Asia-Pacific Power and Energy Engineering Conference* (pp. 1–4). IEEE.

Moradijoz, M., & Moghaddam, M. P. (2012). Optimum allocation of parking lots in distribution systems for loss reduction. In *2012 IEEE Power and Energy Society General Meeting* (pp. 1–5). IEEE.

Networking and Emerging Optimization. (n.d.). Capacitated VRP Instances | Vehicle Routing Problem. Retrieved December 6, 2017, from http://neo.lcc.uma.es/vrp/vrp-instances/capacitated-vrp-instances/

Neyestani, N., Damavandi, M. Y., Shafie-khah, M., Catalao, J. P. S., & Contreras, J. (2014). Allocation of PEVs' Parking lots in renewable-based distribution system. In *2014 Australasian Universities Power Engineering Conference (AUPEC)* (pp. 1–6). IEEE.

Neyestani, N., Damavandi, M. Y., Shafie-Khah, M., Contreras, J., & Catalao, J. P. S. (2015). Allocation of Plug-In Vehicles' Parking Lots in Distribution Systems Considering Network-Constrained Objectives. *IEEE Transactions on Power Systems*, *30*(5), 2643–2656.

Pallottino, S., & Scutellà, M. G. (1998). Shortest Path Algorithms In Transportation Models: Classical and Innovative Aspects. In *Equilibrium and Advanced Transportation Modelling* (pp. 245–281). Boston, MA: Springer US. https://doi.org/10.1007/978-1-4615-5757-9_11

Pazouki, S., Mohsenzadeh, A., Ardalan, S., & Haghifam, M.-R. (2015). Simultaneous Planning of PEV Charging Stations and DGs Considering Financial, Technical,and Environmental Effects. *Canadian Journal of Electrical and Computer Engineering*, *38*(3), 238–245.

Pazouki, S., Mohsenzadeh, A., Haghifam, M.-R., & Ardalan, S. (2015). Simultaneous Allocation of Charging Stations and Capacitors in Distribution Networks Improving Voltage and Power Loss. *Canadian Journal of Electrical and Computer Engineering*, *38*(2), 100–105.

Pourazarm, S., Cassandras, C. G., & Malikopoulos, A. (2014). Optimal routing of electric vehicles in networks with charging nodes: A dynamic programming approach. In *2014 IEEE International Electric Vehicle Conference (IEVC)* (pp. 1–7). IEEE. https://doi.org/10.1109/IEVC.2014.7056110

Power Systems Planning Group. (n.d.). EVCS location problem considering CVRP and SP problem for freight transportation. Retrieved June 2, 2017, from http://academia.utp.edu.co/planeamiento/sistemas-de-prueba/recarga-de-vehiculos-electricos-en-sistemas-de-distribucion-3/

Qian, K., Zhou, C., Allan, M., & Yuan, Y. (2011). Effect of load models on assessment of energy losses in distributed generation planning. *International Journal of Electrical Power & Energy Systems*, *33*(6), 1243–1250.

Sarrafan, K., Sutanto, D., Muttaqi, K. M., & Town, G. (2016). Accurate range estimation for an electric vehicle including changing environmental conditions and traction system efficiency. *IET Electrical Systems in Transportation*, *7*(2), 117–124. Retrieved from http://digital-library.theiet.org/content/journals/10.1049/iet-est.2015.0052

Schmidt, E. (2017). 2017 Battery Electric Cars Reported Range Comparison. Retrieved December 13, 2017, from https://www.fleetcarma.com/2017-battery-electric-cars-reported-range-comparison/

Su, C. L., Leou, R. C., Yang, J. C., & Lu, C. N. (2013, November). Optimal electric vehicle charging stations placement in distribution systems. In *IECON 2013-39th Annual Conference of the IEEE Industrial Electronics Society*(pp. 2121-2126). IEEE.

Tesla Motors. (2017). Tesla Supercharger. Retrieved June 1, 2017, from https://www.tesla.com/supercharger

Toro, E. M., Franco, J. F., Echeverri, M. G., & Guimarães, F. G. (2017). A multi-objective model for the green capacitated location-routing problem considering environmental impact. *Computers & Industrial Engineering*, *110*, 114–125.

Toth, P., Vigo, D., Burkard, R. E., Glover, F., Hoffman, A. J., Karoski, M., … Welsh, D. J. A. (n.d.). THE VEHICLE ROUTING PROBLEM Editorial Board Evaluation and Optimization of Electoral Systems. *J. P*. Retrieved from http://www.siam.org/journals/ojsa.php

U.S. Department of Energy. (2017). Alternative Fuels Data Center: Charging Plug-In Electric Vehicles at Home. Retrieved June 1, 2017, from https://www.afdc.energy.gov/fuels/electricity_charging_home.html

Wang, S., Dong, Z. Y., Luo, F., Meng, K., & Zhang, Y. (2017). Stochastic Collaborative Planning of Electric Vehicle Charging Stations and Power Distribution System. *IEEE Transactions on Industrial Informatics*, 1–1.

Worley, O., Klabjan, D., & Sweda, T. M. (2012). Simultaneous vehicle routing and charging station siting for commercial Electric Vehicles. In *IEEE International Electric Vehicle Conference* (pp. 1–3).

Xie, F., Huang, M., Zhang, W., & Li, J. (2011). Research on electric vehicle charging station load forecasting. In *2011 International Conference on Advanced Power System Automation and Protection* (pp. 2055–2060). IEEE.

Yang, H., Pan, H., Luo, F., Qiu, J., Deng, Y., Lai, M., & Dong, Z. Y. (2017). Operational Planning of Electric Vehicles for Balancing Wind Power and Load Fluctuations in a Microgrid. *IEEE Transactions on Sustainable Energy*, *8*(2), 592–604.

Zheng, Y., Dong, Z. Y., Xu, Y., Meng, K., Zhao, J. H., & Qiu, J. (2014). Electric Vehicle Battery Charging/Swap Stations in Distribution Systems: Comparison Study and Optimal Planning. *IEEE Transactions on Power Systems*, *29*(1), 221–229.

Zhang, H., Hu, Z., Xu, Z., & Song, Y. (2016). An Integrated Planning Framework for Different Types of PEV Charging Facilities in Urban Area. *IEEE Transactions on Smart Grid*, *7*(5), 2273–2284.

Zhang, H., Hu, Z., Xu, Z., & Song, Y. (2017). Optimal Planning of PEV Charging Station With Single Output Multiple Cables Charging Spots. *IEEE Transactions on Smart Grid*, *8*(5), 2119–2128.